Theory of chemically-induced dynamic spin polarization. IV. Low-field effects[a)]

Gary P. Zientara and Jack H. Freed[b)]

Department of Chemistry, Cornell University, Ithaca, New York 14853
(Received 28 August 1978)

The Pedersen–Freed theory of chemically-induced dynamic spin polarization is extended to low field cases where the $T_{\pm} \rightarrow S$ transitions must be included. The solutions of the stochastic-Liouville equation are again obtained by numerical finite-difference (FD) methods, but order of magnitude reductions in the size of the matrices to be inverted are realized by introduction of a simple modification of the FD expressions. The simplest case of a single nuclear spin of $I = 1/2$ on one radical is treated in detail. The results show unequivocally the significant dependence of both CIDNP and CIDEP signals on both the magnitude and the range of the exchange interaction. Also, significant polarizations which should be observable are predicted for both types of experiment under appropriate low field conditions. All the computed results are consistent with a simple qualitative model involving two primary regions in r space: in the outer region the hyperfine terms induce $T_{\pm} \rightarrow S$ transitions and $J(r) = 0$, while in the inner region $J(r)$ modulates the effectiveness of these transitions. Consideration is also given to magnetic-field effects on chemical reactivity as well as $T_{\pm} \rightarrow S$ contributions in high field but viscous CIDEP.

I. INTRODUCTION

The theory of chemically-induced dynamic nuclear (CIDNP) and electron (CIDEP) polarizations in high magnetic fields has been extensively studied in the past by use of the stochastic-Liouville approach.[1,2] Our formulation relies on numerical finite-difference (FD) calculations applied to the solution of the stochastic-Liouville equation (SLE) and provides the ability to include in various models a physically realistic exchange interaction ($J(r)$), Coulombic forces, exchange forces, and hydrodynamic effects. The results of numerical computation of high field CIDNP signal intensities were found to be not very sensitive to $J(r)$,[1a,e] and therefore the problem could be simplified, yielding solutions less dependent on numerical methods.[3] High-field CIDEP signal enhancements were shown to be strongly dependent on the magnitude and spatial extent of $J(r)$, for which numerical solutions are required. The following results and discussion reveal that, as others have conjectured,[4] the exchange interaction can play a large role in determining *both* CIDNP and CIDEP signal intensities in low-field cases, where there are $S - T_{\pm}$ couplings (as well as $S - T_0$) among the electron spin states of a radical pair.

The present calculation of representative CIDN(E)P signal enhancements in low magnetic fields is based on the application of the SLE according to the theory of Pedersen and Freed[1] where an exchange interaction of finite extent, $J(r)$, between the two radicals is included.

Past CIDNP studies by other workers have attempted low-field solutions by making one of several approximations in order to circumvent the problem of noncommuting spin–Hamiltonian and diffusion operators. These approximations focused on $J(r)$, the only spatially dependent portion of the spin–Hamiltonian, approximating it as a constant during a period when the radicals diffuse to within a certain distance of each other,[5] or as a constant throughout all space,[6,7] or as a constant only during radical contact[8] ("contact exchange" model). All such theories tried to account for the large difference in experimental NMR signal intensities[4,6–10] observed from reaction products created in low magnetic fields (0–~100 G) compared to those formed in high magnetic fields ($\gtrsim$3500 G). Some low-field signals were observed to switch from absorption to emission (or vice versa) as a function of the magnetic field during reaction,[7,10] thus indicating the presence of a complex nuclear spin-mixing process. This nuclear spin polarization scheme must include the electronic $m_s = \pm 1$ triplet (T_+, T_-) states (involved in nuclear spin polarization via actual proton spin flips due to the hyperfine term). These states are usually neglected in high-field theories due to their large Zeeman energy separations from the $m_s = 0$ singlet (S) and triplet (T_0) states. (The $S - T_0$ mixing does not directly cause nuclear polarization but does yield product polarization as a result of spin selective recombination reactions.[6])

The analogous CIDEP effects coming from reactions carried out in low magnetic fields or under special physical conditions are similarly dependent on $S - T_{\pm}$ coupling effects. Experimental ESR spectral intensities observed from certain systems have been proposed as due to $S - T_{\pm}$ mixing.[11] There has only been one attempt to calculate the magnitude of low-field CIDEP effects, but in terms of a simple, approximate analysis.[5]

A primary problem with applying the SLE–FD method to the complete problem involving all electron spin states, S, T_0, $T_{\pm}$ of the interacting radical pair (as well as the nuclear-spin states) is the large increase in the order of the matrix to be inverted. Thus, we have focused on the development of new computing algorithms, which can be used for such problems, and some of them have been summarized recently.[2] In this work we employ a relatively simple modification of the FD equations used by Pedersen and Freed,[1] which leads to order-of-magnitude reductions in the size of the matrices involved in the solutions yet yielding *increased* numerical accuracy in the results.

II. THEORETICAL AND NUMERICAL ASPECTS

The matrix elements for the spin Hamiltonian, $\mathcal{H}(r)$, for the relatively simple but instructive case of interacting radicals one of which has no nuclear spins, while

[a)]Supported by NSF Grant CHE77-26996.
[b)]Partially supported by a NATO Research grant.

 0021-9606/79/031359-12$01.00

the other has a nuclear spin I, has been given previously.[2] We repeat it here for purposes of reference in the discussion. We class the combined electronic and nuclear-spin states by $|i, M_I\rangle$ where $i = S$, T_0, or $T_\pm$, while M_I is the nuclear-spin quantum number. Then, in this basis $\mathcal{H}(r)$ may be written as:

$\|S, M_I\rangle$	$\|T_0, M_I\rangle$	$\|T_+, M_I-1\rangle$	$\|T_-, M_I+1\rangle$
$2J(r)$	Q	$-B^-$	B^+
Q	0	B^-	B^+
$-B^-$	B^-	C^-	0
B^+	B^+	0	$-C^+$

, (2.1)

where:

$$Q \equiv \tfrac{1}{2}(g_a - g_b)\beta_e\hbar^{-1}B_0 + \tfrac{1}{2}A_a M_I \tag{2.2a}$$

$$B^\pm \equiv \frac{1}{\sqrt{8}} A_a[I(I+1) - M_I(M_I \pm 1)]^{1/2} \tag{2.2b}$$

$$C^\pm \equiv \tfrac{1}{2}(g_a + g_b)\beta_e\hbar^{-1}B_0 + \tfrac{1}{2}A_a(M_I \pm 1)\,, \tag{2.2c}$$

where the terms in Eqs. (2.2) are as used previously [cf. glossary of symbols in Ref. 1(a)]. We will assume here that the single nuclear spin is $I = \frac{1}{2}$ (e.g., a proton) residing on radical a. Thus $\mathcal{H}(r)$ will lead to two sets of uncoupled spin manifolds: (1) $|S, +\rangle$, $|T_0, +\rangle$, and $|T_+, -\rangle$, which we refer to as the $M_I = \frac{1}{2}$ manifold (since we are particularly interested in the S states, see below); and (2) $|S, -\rangle$, $|T_0, -\rangle$, and $|T_-, +\rangle$ referred to as the $M_I = -\frac{1}{2}$ manifold. [Below we let $|S, \pm\rangle = S(\pm)$, $|T_0, \pm\rangle = T_0(\pm)$, $|T_\pm, \mp\rangle = T_\pm(\mp)$.]

As before, we make use of dimensionless parameters for more compact analyses; thus we define the dimensionless distance $y \equiv r/d$ (r = radial radical separation, d = distance of closest approach of the two nuclei).[12] In a FD format we can discretize space into N nodes (with index $i = 1$ to N) with each node at distance y_i ($y_1 = 1$) from the origin. Also, we will make use of a variable internodal separation through *all* of space unlike past numerical studies.[1,2] This separation is defined as $h^{(i)} \equiv y_{i+1} - y_i$ for $1 \le i \le N-1$ and, as has proven successful in another numerical study of CIDN(E)P,[13] we will employ a geometrically increasing $h^{(i)}$ such that:

$$h^{(1)} \equiv \Delta_I \tag{2.3a}$$

$$h^{(i)} \equiv \Delta_I \Delta_0^{i-1} \tag{2.3b}$$

so

$$y_i = 1 + \sum_{j=1}^{i-1} h^{(j)} \quad \text{for } i > 1\,. \tag{2.4}$$

This choice can be included in the general FD equations for the diffusive portion of the CIDN(E)P problem having an inner reflecting wall boundary condition and an outer "collecting" region. The transition matrix, **W**, the FD analogue of the radial diffusion operator, $\partial^2/\partial y^2$, for variable nodal separation is:

$$W_{1,1} = -2(1 + h^{(1)})/(h^{(1)}h^{(1)}) \tag{2.5a}$$

$$W_{1,2} = +2/(h^{(1)}h^{(1)}) \tag{2.5b}$$

and for $1 < i < N$

$$W_{i,i-1} = +2/[h^{(i-1)}(h^{(i)} + h^{(i-1)})] \tag{2.5c}$$

$$W_{i,i} = -2/(h^{(i)}h^{(i-1)}) \tag{2.5d}$$

$$W_{i,i+1} = +2/[h^{(i)}(h^{(i)} + h^{(i-1)})] \tag{2.5e}$$

except for

$$W_{N,N-1} = +2/(h^{(N-1)}h^{(N-1)}) \tag{2.6a}$$

$$W_{N-1,N} = W_{N,N} = 0 \tag{2.6b}$$

with all other

$$W_{i,j} = 0\,. \tag{2.7}$$

The FD volume elements,[1] analogues of the differential form $y dy$ become:

$$V_i = y_i(h^{(i)} + h^{(i-1)})/2 \tag{2.8a}$$

except for

$$V_1 = h^{(1)}/2 \tag{2.8b}$$

$$V_N = y_N h^{(N-1)}/2\,. \tag{2.8c}$$

Although these Eqs. (2.5)–(2.8) are suitable for any functional choice for $h^{(i)}$, the advantage of using a geometrically increasing internodal distance is its rather fine graining in the interior region where the diffusive motion influences the effect of $J(r)$ on the system, while the coarse graining in the outer region allows for a physical problem of great extent ($y_N \sim 3\times10^4$ used in this work) which is represented with as few as 50 nodal positions (i.e., $N = 50$). This offers a great computational benefit over past numerical studies (where $N \approx 400$ was often used) and yields computer programs for CIDN(E)P solutions which may be implemented on a minicomputer. This work was performed on a PDP 11/34 minicomputer with matrix inversion by Gaussian elimination with pivoting.

The quantum mechanical behavior of the relevant spin states noted above follows from Eq. (2.1). Here we shall refer to the dimensionless quantities $a \equiv A_a d^2/D$ (the hyperfine constant), $J(y)d^2/D = (J_0 d^2/D) \times \exp[-\lambda d(y-1)]$ (the exchange interaction) with $\lambda = 5\ln 10/r_{ex}$, kd^2/D (the reaction rate constant), $\sigma \equiv sd^2/D$ (the Laplace transform variable), and $g\beta_e\hbar^{-1}B_0 d^2/D$ (the electronic Zeeman term). $\tau_1(\lambda)D/d^2$ is the dimensionless lifetime of the exchanging radical pair, given by Pedersen and Freed[1] as: $\tau_1(\lambda)D/d^2 \approx (\lambda d)^{-1}[1 + (\lambda d)^{-1}]$. All calculations below are for $\Delta g = (g_a - g_b) = 0$ [thus $Qd^2/D = \pm a/4$] with $g_a = g_b \equiv g$, a case suited to our present exploration of the effects of the exchange interaction.[5,7] Spin–lattice relaxation of the individual radicals typically need not be explicitly included in these calculations since it can usually be added at a later stage of the problem by means of the two-time scale approach outlined by Pedersen and Freed.[1] This approach is valid when the polarizations are generated in times short compared to T_1 and T_2, although simple approximate methods exist for including such effects as the time scales become more nearly equal.[1a,14]

Sensible choices of initial conditions would be singlet initial (S.I.), triplet initial (T.I.)[15] or random initial (R.I.) as before,[1] but where the $M_I = \pm\frac{1}{2}$ nuclear states are equally probable. Thus we write S.I. as: $\rho_{S(-)} = \rho_{S(+)} = \frac{1}{2}$; while T.I. is: $\rho_{T_+(-)} = \rho_{T_-(+)} = \rho_{T_0(\pm)} = \frac{1}{6}$ (while the $\rho_{T_+(+)} = \rho_{T_-(-)}$, which directly participate in the CIDEP polarization process and may affect both CIDN(E)P indirectly via T_1 and T_2 [cf. 1(a) and below], also are initially $\frac{1}{6}$ each); the R.I. case corresponds to

a value of $\frac{1}{8}$ for each of the eight diagonal-density matrix elements. In all cases, we assume random initial phases.[1] Our notation is to write a diagonal-density-matrix element as $\rho_i(\pm)$ where i refers to the electron-spin state of the radical pair and $\pm$ refers to $M_I = \pm\frac{1}{2}$.

In this work we have assumed that the radical-pair forms from an excited triplet state of the dissociating molecule[15] and the spin-dependent reactivity requires a singlet state for recombination. We then have that the experimental CIDNP enhancement from the recombination product for the $I=\frac{1}{2}$ system is[1]:

$$V^{\exp}_{(\mathrm{CIDNP})} \propto \Delta\mathcal{F}/(P^{eq}_{+} - P^{eq}_{-})\mathcal{F} \ , \tag{2.9}$$

where $P^{eq}_{\pm}$ is the equilibrium Boltzmann factor for the $M_I = \pm\frac{1}{2}$ state:

$$P^{eq}_{\pm} = \frac{\exp(\pm\frac{1}{2}g_N\beta_N\hbar^{-1}B_0/kT)}{\sum_{M_I}\exp(M_I g_N\beta_N\hbar^{-1}B_0/kT)} \cong \frac{1 \pm \frac{1}{2}g_N\beta_N\hbar^{-1}B_0/kT}{2} \tag{2.10}$$

and where

$$\mathcal{F} = \mathcal{F}_{+} + \mathcal{F}_{-} \tag{2.11a}$$

$$\Delta\mathcal{F} = \mathcal{F}_{+} - \mathcal{F}_{-} \tag{2.11b}$$

$$\mathcal{F}_{\pm} = \mathcal{P}_{\pm}(t=0) - \mathcal{P}_{\pm}(t=\infty) \tag{2.11c}$$

while $\mathcal{F}_{\pm}$ correspond to the total probability of reaction for the radical pair per collision from the $M_I = \pm\frac{1}{2}$ nuclear state (and singlet electron-spin state) and $\mathcal{P}_{\pm}(t)$ is the total probability within the respective spin manifold [$\mathcal{P}_{\pm}(t=0) = \frac{1}{8}$ for random T. I.]. We note in the high-field limit of the present case, $I=\frac{1}{2}$ and $\Delta g = 0$, the result $\mathcal{F}_{+} = \mathcal{F}_{-}$ (since only $S - T_0$ mixing occurs in both manifolds) so that $\Delta\mathcal{F} = 0$. Thus, the value of $\Delta\mathcal{F}$ is a good measure of the contributions from the $T_{\pm}$ states (or in other words the "low-field" correction). It follows then that our example is well-chosen to demonstrate the existence of low-field effects.

It was shown in Refs. 1 that for CIDNP it is useful to define the reactivity Λ as the total probability of reaction per collision (assuming S. I. and zero spin-polarizing contribution) as well as $\mathcal{F}^* \equiv \lim_{\Lambda\to 1}\mathcal{F}(\mathrm{T.\,I.})$, which measures the conversion from triplets to singlets for the whole reaction. We define $\mathcal{F}^*$ and $\Delta\mathcal{F}^*$ analogously (as well as $\mathcal{F}^*_{\pm}$) as the $\Lambda \to 1$ limit. It was shown in Refs. 1 that a relationship exists between $\mathcal{F}$ and the Λ and $\mathcal{F}^*$ based on statistical arguments which were confirmed in detail by the computed results. The generalization to the present case of random T. I. is (for each of the two uncoupled sets of spin manifolds):

$$\mathcal{F}_{\pm} = \Lambda\mathcal{F}^*_{\pm}[1 + 6\mathcal{F}^*_{\pm}(1-\Lambda)]^{-1} \ , \tag{2.12}$$

which has again been confirmed by computed results.

For CIDEP (and $I=\frac{1}{2}$), the electron-spin polarization may be related to the observed signal enhancement, V, by:

$$V_{a(\pm)}(\mathrm{CIDEP}) \propto P^{\infty}_{a(\pm)}(\mathrm{T.\,I.})/P_{eq} \tag{2.13a}$$

$$V_b(\mathrm{CIDEP}) \propto \tfrac{1}{2}[P^{\infty}_{b(+)}(\mathrm{T.\,I.}) + P^{\infty}_{b(-)}(\mathrm{T.\,I.})]/P_{eq} \tag{2.13b}$$

with $P_{eq} \cong \frac{1}{2}g_e\beta_e\hbar^{-1}B_0/kT$ the equilibrium electron-spin polarization, and where $P^{\infty}_{a(\pm)}$ refer to the polarizations from the $M_I = \pm\frac{1}{2}$ nuclear states i. e., [1]:

$$P_{a(\pm)} = -[\rho_{S(\pm),T_0(\pm)} + \rho_{T_0(\pm),S(\pm)}] + [\rho_{T_-(\pm)} - \rho_{T_+(\pm)}] \tag{2.14a}$$

while

$$P_{b(\pm)} = +[\rho_{S(\pm),T_0(\pm)} + \rho_{T_0(\pm),S(\pm)}] + [\rho_{T_-(\pm)} - \rho_{T_+(\pm)}] \ , \tag{2.14b}$$

which may be analyzed more effectively by separation into the specific terms $P_{\mathrm{HF}(\pm)}$ and $P_{\mathrm{LF}(\pm)}$,

$$P_{\mathrm{HF}(\pm)} = \rho_{S(\pm),T_0(\pm)} + \rho_{T_0(\pm),S(\pm)} \tag{2.14c}$$

$$P_{\mathrm{LF}(\pm)} = \rho_{T_-(\pm)} - \rho_{T_+(\pm)} \ . \tag{2.14d}$$

$P_{\mathrm{HF}(\pm)}$ represents the portion of the polarization which remains nonzero at high magnetic field (if Q, $J_0 \neq 0$) while the $P_{\mathrm{LF}(\pm)}$ are typically nonzero only in low magnetic fields. As before, the superscript ∞ will be used to refer to the $t \to \infty$ limit of the respective polarization. Also, as in Refs. 1, an exact relationship may be written between $P^{\infty}_{a(\pm)}(\mathrm{T.\,I.})$, $P^{\infty}_{b(\pm)}(\mathrm{T.\,I.})$ [or $P^{\infty}_{\mathrm{HF}(\pm)}, P^{\infty}_{\mathrm{LF}(\pm)}$] and the values of $\mathcal{F}^*_{\pm}$, Λ and the polarization calculated when $\Lambda = 0$. Hence, we have the following relations[16] confirmed by actual numerical results,

$$P^{\infty}_{a(\pm)}(\mathrm{T.\,I.}, \Lambda \neq 0) = -\mathcal{G}_{\pm}P^{\infty}_{\mathrm{HF}(\pm)}(\mathrm{T.\,I.}, \Lambda = 0) + \mathcal{G}_{\mp}P^{\infty}_{\mathrm{LF}(\pm)}(\mathrm{T.\,I.}, \Lambda = 0) \tag{2.15a}$$

$$P^{\infty}_{b(\pm)}(\mathrm{T.\,I.}, \Lambda \neq 0) = \mathcal{G}_{\pm}P^{\infty}_{\mathrm{HF}(\pm)}(\mathrm{T.\,I.}, \Lambda = 0) + \mathcal{G}_{\mp}P^{\infty}_{\mathrm{LF}(\pm)}(\mathrm{T.\,I.}, \Lambda = 0) \tag{2.15b}$$

where

$$\mathcal{G}_{\pm} \equiv [1 + 6\mathcal{F}^*_{\pm}][1 + (1-\Lambda)6\mathcal{F}^*_{\pm}]^{-1} \ . \tag{2.15c}$$

Equations (2.12) and (2.15) are specific to the random triplet initial condition (i. e., $\rho_{T_0(\pm)} = \rho_{T_{\pm}(\mp)} = \frac{1}{8}$) and therefore include the necessary numerical factors. The coefficient of the $P^{\infty}_{\mathrm{LF}(\pm)}$ term is $\mathcal{G}_{\mp}$ rather than $\mathcal{G}_{\pm}$ since the triplet (± 1) state influencing $P^{\infty}_{a(\pm)}$ [or $P^{\infty}_{b(\pm)}$] enters from the other uncoupled spin manifold, which possesses a different triplet to singlet transition probability. Thus, it is only necessary to compute the results $P^{\infty}_{\mathrm{HF}(\pm)}$ and $P^{\infty}_{\mathrm{LF}(\pm)}$ for $\Lambda = 0$, from which the experimentally observable quantities may be calculated via Eqs. (2.13)–(2.15).

We now introduce the notation:

$$P^{\infty}_{a} = P^{\infty}_{a(+)} + P^{\infty}_{a(-)} \tag{2.16a}$$

$$P^{\infty}_{b} = P^{\infty}_{b(+)} + P^{\infty}_{b(-)} \ . \tag{2.16b}$$

We note that P^{∞}_{a} will be zero in the high-field limit (for this $I=\frac{1}{2}$, $\Delta g = 0$ case) when only $S - T_0$ mixing is important. Thus P^{∞}_{a} is a measure of the total contributions from the $T_{\pm}$ states [cf. Eqs. (2.1) and (2.14)]. Similarly, P^{∞}_{b} yields the high-field result of zero in each example when only $S - T_0$ mixing is important and one notes that for $\Delta g = 0$ Qd^2/D $(M_I = \frac{1}{2}) = -Qd^2/D$ $(M_I = -\frac{1}{2}) = a/4$. Thus, in high magnetic fields[1] $P^{\infty}_{a(+)} = -P^{\infty}_{a(-)}$ and $P^{\infty}_{b} = 0$ since $P^{\infty}_{\mathrm{HF}(+)} = -P^{\infty}_{\mathrm{HF}(-)}$.

III. CIDNP RESULTS

The quantity $\Delta\mathcal{F}^*$, important for CIDNP, is shown in Table I and Fig. 1 as a function of magnetic field for a range of values of $j_0 = J_0d^2/D$ and $a(=A_ad^2/D)$. These results can be extended by using

$$\mathcal{F}^*(A_a, J_0, \Delta g = 0) = \mathcal{F}^*(-A_a, -J_0, \Delta g = 0) \tag{3.1a}$$

$$\Delta\mathcal{F}^*(A_a, J_0, \Delta g = 0) = -\Delta\mathcal{F}^*(-A_a, -J_0, \Delta g = 0) \ . \tag{3.1b}$$

It can be immediately noted that the magnitude and sign of j_0 causes wide variation in $\Delta\mathcal{F}^*$, and thus the ob-

TABLE I. $\Delta\mathfrak{F}^* \times 10^3$ ($\mathfrak{F}^* \times 10^3$), [a–c]

B_0 (Gauss)	$A_a d^2/D = 0.064$ $J_0 d^2/D = 160.0$ $2J_0\tau_1(\lambda) = 30.1$	$A_a d^2/D = 0.064$ $J_0 d^2/D = 16.0$ $2J_0\tau_1(\lambda) = 3.01$	$A_a d^2/D = 0.064$ $J_0 d^2/D = 1.60$ $2J_0\tau_1(\lambda) = 0.301$	$A_a d^2/D = 0.064$ $J_0 d^2/D = 0.160$ $2J_0\tau_1(\lambda) = 0.030$	$A_a d^2/D = 0.064$ $J_0 d^2/D = 0.016$ $2J_0\tau_1(\lambda) = 0.003$	$A_a d^2/D = 0.064$ $J_0 d^2/D = 0.0$ $2J_0\tau_1(\lambda) = 0.0$
0	0.0 (20.1)	0.0 (19.8)	0.0 (21.8)	0.0 (22.8)	0.0 (22.9)	0.0 (22.9)
1	0.37(22.4)	0.41(22.2)	0.50(24.4)	0.48(25.3)	0.48(25.4)	0.48(25.4)
5	1.41(24.8)	1.63(24.8)	1.97(27.3)	1.86(28.1)	1.85(28.1)	1.84(28.1)
10	2.16(25.7)	2.54(25.8)	3.04(28.4)	2.82(29.1)	2.79(29.1)	2.79(29.1)
15	2.49(25.7)	2.97(25.9)	3.49(28.4)	3.21(29.0)	3.17(29.0)	3.17(29.0)
20	2.57(25.2)	3.09(25.5)	3.57(27.9)	3.26(28.4)	3.22(28.4)	3.21(28.4)
25	2.51(24.7)	3.04(25.0)	3.46(27.3)	3.14(27.7)	3.10(27.7)	3.10(27.7)
30	2.40(24.1)	2.92(24.4)	3.27(26.7)	2.96(27.0)	2.92(27.0)	2.91(27.0)
35	2.26(23.6)	2.76(24.0)	3.05(26.1)	2.75(26.4)	2.72(26.4)	2.71(26.4)
40	2.12(23.1)	2.59(23.5)	2.83(25.6)	2.55(25.8)	2.52(25.8)	2.52(25.8)
45	1.98(22.7)	2.43(23.1)	2.63(25.2)	2.37(25.4)	2.34(25.4)	2.34(25.4)
50	1.86(22.4)	2.28(22.8)	2.44(24.8)	2.20(25.0)	2.18(25.0)	2.17(25.0)
55	1.74(22.1)	2.14(22.5)	2.27(24.5)	2.05(24.7)	2.03(24.7)	2.02(24.7)
60	1.63(21.9)	2.01(22.3)	2.12(24.2)	1.92(24.4)	1.90(24.4)	1.89(24.4)
65	1.54(21.6)	1.90(22.1)	1.99(24.0)	1.80(24.2)	1.78(24.2)	1.77(24.2)
70	1.45(21.5)	1.79(21.9)	1.87(23.8)	1.69(24.0)	1.67(24.0)	1.67(24.0)
75	1.37(21.3)	1.70(21.7)	1.76(23.6)	1.59(23.8)	1.58(23.8)	1.57(23.8)
80	1.30(21.2)	1.61(21.6)	1.66(23.5)	1.51(23.6)	1.49(23.6)	1.49(23.6)
85	1.24(21.0)	1.53(21.5)	1.57(23.3)	1.43(23.5)	1.41(23.5)	1.41(23.5)
90	1.18(20.9)	1.46(21.4)	1.49(23.2)	1.36(23.4)	1.34(23.4)	1.34(23.4)
95	1.13(20.8)	1.40(21.3)	1.42(23.1)	1.29(23.3)	1.28(23.3)	1.28(23.3)
100	1.08(20.7)	1.34(21.2)	1.35(23.0)	1.23(23.2)	1.22(23.2)	1.22(23.2)
150	0.74(20.2)	0.93(20.6)	0.91(22.5)	0.84(22.7)	0.83(22.7)	0.83(22.7)

B_0 (Gauss)	$A_a d^2/D = 0.064$ $J_0 d^2/D = -0.016$ $2J_0\tau_1(\lambda) = -0.003$	$A_a d^2/D = 0.064$ $J_0 d^2/D = -0.160$ $2J_0\tau_1(\lambda) = -0.030$	$A_a d^2/D = 0.064$ $J_0 d^2/D = -1.60$ $2J_0\tau_1(\lambda) = -0.301$	$A_a d^2/D = 0.064$ $J_0 d^2/D = -16.0$ $2J_0\tau_1(\lambda) = -3.01$	$A_a d^2/D = 0.064$ $J_0 d^2/D = -160.0$ $2J_0\tau_1(\lambda) = -30.1$
0	0.0 (22.9)	0.0 (23.0)	0.0 (23.8)	0.0 (22.3)	0.0 (21.0)
1	0.47(25.5)	0.47(25.5)	0.43(26.2)	0.31(24.4)	0.33(23.2)
5	1.84(28.2)	1.83(28.2)	1.62(28.7)	1.12(26.6)	1.23(25.5)
10	2.79(29.1)	2.76(29.2)	2.41(29.5)	1.62(27.3)	1.83(26.2)
15	3.16(29.0)	3.12(29.0)	2.69(29.3)	1.78(27.0)	2.07(26.1)
20	3.21(28.4)	3.17(28.4)	2.71(28.6)	1.77(26.4)	2.10(25.6)
25	3.09(27.7)	30.5(27.7)	2.60(27.8)	1.69(25.7)	2.03(24.9)
30	2.91(27.0)	2.87(27.0)	2.44(27.0)	1.57(25.0)	1.92(24.3)
35	2.71(26.4)	2.67(26.4)	2.27(26.4)	1.46(24.4)	1.80(23.7)
40	2.51(25.8)	2.48(25.8)	2.11(25.8)	1.35(23.9)	1.68(23.2)
45	2.33(25.4)	2.30(25.4)	1.96(25.3)	1.25(23.4)	1.56(22.8)
50	2.17(25.0)	2.14(25.0)	1.83(24.9)	1.16(23.1)	1.46(22.5)
55	2.02(24.7)	2.00(24.7)	1.71(24.6)	1.08(22.7)	1.36(22.2)
60	1.89(24.4)	1.87(24.4)	1.60(24.3)	1.00(22.5)	1.27(21.9)
65	1.77(24.2)	1.75(24.2)	1.51(24.1)	0.94(22.2)	1.20(21.7)
70	1.67(24.0)	1.65(24.0)	1.42(23.9)	0.88(22.0)	1.13(21.5)
75	1.57(23.9)	1.55(23.8)	1.34(23.7)	0.83(21.9)	1.06(21.3)
80	1.49(23.7)	1.47(23.7)	1.27(23.5)	0.79(21.7)	1.01(21.2)
85	1.41(23.5)	1.39(23.5)	1.21(23.4)	0.74(21.6)	0.96(21.1)
90	1.34(23.4)	1.32(23.4)	1.15(23.3)	0.71(21.4)	0.91(21.0)
95	1.28(23.3)	1.26(23.3)	1.10(23.2)	0.67(21.3)	0.87(20.9)
100	1.22(23.2)	1.20(23.2)	1.05(23.1)	0.64(21.2)	0.83(20.8)
150	0.82(22.7)	0.82(22.7)	0.73(22.5)	0.43(20.7)	0.57(20.2)

B_0 (Gauss)	$A_a d^2/D = 0.016$ $J_0 d^2/D = 0.0$ $2J_0\tau_1(\lambda) = 0.0$	$A_a d^2/D = 0.0064$ $J_0 d^2/D = 0.0$ $2J_0\tau_1(\lambda) = 0.0$
0	0.0 (11.5)	0.0 (7.21)
1	0.74(13.7)	0.81(8.99)

TABLE I (*Continued*)

B_0 (Gauss)	$A_a d^2/D = 0.016$ $J_0 d^2/D = 0.0$ $2J_0\tau_1(\lambda) = 0.0$	$A_a d^2/D = 0.0064$ $J_0 d^2/D = 0.0$ $2J_0\tau_1(\lambda) = 0.0$
5	1.53(14.0)	0.65(7.77)
10	1.21(12.8)	0.37(7.21)
15	0.92(12.1)	0.25(7.04)
20	0.73(11.7)	0.19(6.96)
25	0.60(11.5)	0.16(6.92)
30	0.50(11.3)	0.13(6.89)
35	0.44(11.2)	0.11(6.87)
40	0.38(11.2)	0.10(6.86)
45	0.34(11.1)	0.09(6.85)
50	0.31(11.1)	0.08(6.85)
55	0.28(11.1)	0.07(6.84)
60	0.26(11.0)	0.07(6.84)
65	0.24(11.0)	0.06(6.83)
70	0.22(11.0)	0.06(6.83)
75	0.21(11.0)	0.05(6.83)
80	0.20(11.0)	0.05(6.83)
85	0.18(11.0)	0.05(6.82)
90	0.17(10.9)	0.04(6.82)
95	0.16(10.9)	0.04(6.82)
100	0.16(10.9)	0.04(6.82)
150	0.10(10.9)	0.03(6.81)

[a] $\Delta\mathfrak{F}^* \times 10^3$ is shown first, with $\mathfrak{F}^* \times 10^3$ following in parenthesis. $\Delta\mathfrak{F}^* > 0$ implies an absorption signal.
[b] Finite difference results found using $\Delta g = 0$, $(g_a + g_b)\, d^2/D = 6.4 \times 10^{-10}$, $\sigma = 10^{-15}$, $\Delta_I = 0.03125$, $\Delta_0 = 1.295$, $N = 50$, $r_N/d = 33593$, $kd^2/D = 10^{20}$ ($\Lambda \cong 1$), $y_{ex} = 1.0$, and random triplet initial condition.
[c] Analytic high field results from J. Pedersen (Ref. 3) adapted to our input with $A_a d^2/D = 0.064$, 0.016, and 0.0064 yield $\mathfrak{F}^* \times 10^3 = 21.9$, 10.8, and 6.78, respectively, for that limiting case (of $B_0 \gtrsim 10^3$). Note that the analytic results of Pedersen are rigorous for $J(r) = 0$ and S-T_0 coupling only.

served NMR signal intensity. In our example, for an exchange interaction of reasonable extent, we find the polarization *only* carries the sign of a, and thus for $a > 0$ and T. I. one obtains an absorption signal with an emission signal for $a < 0$ and T. I. All signs of $\Delta\mathfrak{F}^*$ (and observed signals) are reversed for S. I.[5,8] and need not be emphasized further. This case, where $\Delta g = 0$ and $I = \frac{1}{2}$ (with a single hyperfine interaction), is seen to be sensitive to the magnitude and the range[17] of $J(r)$, and it can easily be treated by the FD approach. The effects of having $J(r) \neq 0$ might not be as obvious[7] if many hyperfine interactions are involved due to the presence of several magnetic nuclei on the radicals.

We are able to summarize all our computed results from a relatively simple point of view, which is illustrated in Fig. 2. Here we have plotted the first-order energy levels from Eq. (2.1) [i.e., let $Q = B^* = 0$ in Eq. (2.1)] vs distance for several representative values of a, j_0, and B_0. Thus $T_0(\pm)$ represents the zero in energy, while the $S(\pm)$ state(s) show a spatial variation in energy due to $J(r)$. That is:

$$E^{(1)}[T_0(\pm)] = 0 \tag{3.2a}$$

$$E^{(1)}[S(\pm)] = 2J(r) \tag{3.2b}$$

$$E^{(1)}[T_+(-)] = -[g\beta_e\hbar^{-1}B_0 - A_a/4] \tag{3.2c}$$

$$E^{(1)}[T_-(+)] = -[g\beta_e\hbar^{-1}B_0 + A_a/4]\,. \tag{3.2d}$$

Each example is characterized by an outer region $y \gg 1$, in which the energy levels correspond to $j_0 = 0$, and in which the hyperfine interaction can effectively induce nuclear-spin and triplet–singlet transitions. We refer to this as the hyperfine-interaction dominated region (HYDOR). The transitions indicated by the arrows show the net effective transition for each region for the T. I. case, so all transitions are shown directed toward the $S(\pm)$ states. [We have noted above that for $\Delta g = 0$ the T_0

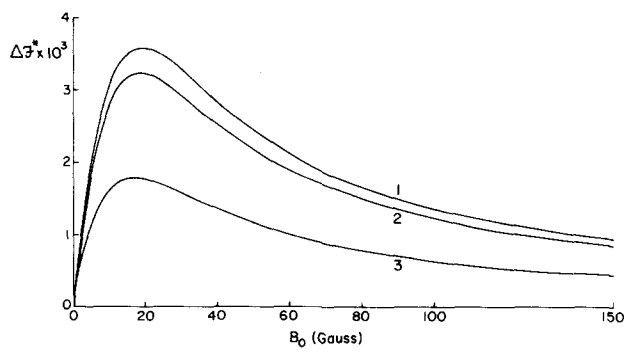

FIG. 1. $\Delta\mathfrak{F}^* \times 10^3$ as a function of the magnetic field, B_0, present during the reaction process. All curves exhibit results for $a = 0.064$. Curve 1 represents results for $j_0 = 1.6$, a case of EIMOR–HYDOR enhancement. Curve 2 is for $j_0 = 0$ illustrating HYDOR effects only. Curve 3 has $j_0 = -16.0$, an example of EIMOR–HYDOR competition. Other input parameters for the calculation of $\Delta\mathfrak{F}^*$ are $\Delta g = 0$, $(g_a + g_b)d^2/D = 6.4 \times 10^{-10}$, $y_{ex} = 1$, $r_N/d = 33593$, $N = 50$, $\Delta_I = 0.03125$, $\Delta_0 = 1.295$, $kd^2/D = 10^{20}$, $\sigma = 10^{-15}$, and a random triplet initial condition.

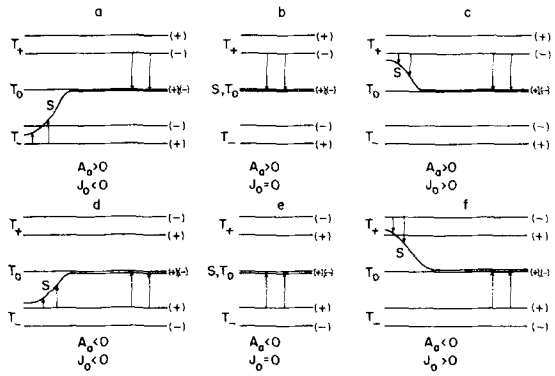

FIG. 2. First-order energy level diagrams for various values of A_a, J_0, and B_0. The vertical axis is energy and the horizontal axis is the interradical separation, which increases from d to ∞ in going from left to right in each diagram. Bracketed signs, (+) or (−), to the right of each energy level refer to the $M_I = \pm\frac{1}{2}$ nuclear state, with the electronic states designated on the left. The arrows indicate the dominant $T_{\pm(\mp)} \rightarrow S_{(\pm)}$ transition in the given region of space. The different figures refer to the various chemical possibilities: (a) EIMOR–HYDOR competition where transitions cause opposing effects and a diminished absorption spectrum for T.I. (relative to the case $J_0 = 0$) or a diminished emission spectrum for S.I. (cf. Fig. 1, curve 3); (b) HYDOR effects only, since $J_0 = 0$. The dominant transition results in an absorption spectrum for T.I. or an emission spectrum for S.I. (cf. Fig. 1, curve 2); (c) EIMOR–HYDOR enhancement, where supporting transitions cause an enhanced absorption spectrum for T.I. (relative to the result for $J_0 = 0$) or an enhanced emission spectrum for S.I.; (d) EIMOR–HYDOR enhancement as in (c) but here producing an enhanced emission spectrum for T.I. or an enhanced absorption spectrum for S.I.; (e) HYDOR effects only. An emission spectrum results for T.I. while an absorption spectrum will result for S.I.; (f) EIMOR–HYDOR competition. A diminished emission spectrum will be observed for T.I. and a diminished absorption spectrum will be found for S.I.

$\rightarrow S$ transitions do not contribute to $\Delta\mathcal{F}$, thus we ignore the transitions $T_-(+) \rightarrow T_0(-)$ and $T_+(-) \rightarrow T_0(+)$ in our simple discussion.] The relative importance of the $T_+(-) \rightarrow S(+)$ vs $T_-(+) \rightarrow S(-)$ transition is determined by whether the magnitude of Eq. (3.1c) is smaller than Eq. (3.1d).

As a result of the spatially varying $J(r)$ there will exist a small region around $y \gtrsim 1$ where the exchange interaction may enhance the rate of one of the transitions: $T_+(-) \rightarrow S(+)$ or $T_-(+) \rightarrow S(-)$ and suppress the other. The transition is still basically induced by the hyperfine term, but the first-order energy levels of Eqs. (3.1) are brought closer for one of the transition pairs (even possibly resulting in a level crossing) and are separated more for the other. This effect depends upon the magnitude of $|j_0|$ as well as the relative signs of j_0 and a. This may be called the exchange-interaction-modulation region (EIMOR), and its effects are thus a function of j_0 and y_{ex} $(= r_{ex}/d)$.

Thus it follows from Eqs. (3.1) that for $a > 0$ the more important transition is $T_+(-) \rightarrow S(+)$; and for $j_0 = 0$ we see in Fig. 1 the positive polarization build up leading to an absorption signal that is due to pure HYDOR effects. For $j_0 > 0$ the EIMOR effect is supportive of the same transition so there is an EIMOR–HYDOR enhancement (relative to the polarization for $j_0 = 0$) which is clearly seen in Fig. 1. This effect appears to be maximized when the energies of the $T_+(-)$ and $S(+)$ states do not differ by too great an amount in the EIMOR, thus it is lost when $j_0 \gg 1$. For $j_0 < 0$ the energy difference between the $T_-(+)$ and $S(-)$ states is narrowed in the inner region, and although there is a buildup of $S(+)$ in the HYDOR, there is a cancelling but somewhat smaller buildup of $S(-)$ via the EIMOR. This can be described as EIMOR–HYDOR competition, and it leads to a diminished signal (relative to the case for $j_0 = 0$). This competition effect is maximized when the energy difference between the $T_-(+)$ and $S(-)$ states is small throughout the EIMOR. Also, the competition is dependent on the magnitude of the EIMOR.

The results for $a < 0$ can be explained by a similar analysis. EIMOR–HYDOR competition exists when $j_0 > 0$, where one may note the effect of the EIMOR-enhanced $T_+(-) \rightarrow S(+)$ transition vs the HYDOR-enhanced $T_-(+) \rightarrow S(-)$ dominant transition. Analogous to the result noted above, the competition is now maximized when the $T_+(-)$ and $S(+)$ states have energies that differ by little in the EIMOR. When $j_0 < 0$ there is EIMOR–HYDOR enhancement, maximized when the $T_-(+)$ and $S(-)$ states have about the same energy value throughout the EIMOR.

In order to test this EIMOR–HYDOR model we have attempted to vary their relative importance for the case of $a > 0$ and $j_0 < 0$ corresponding to an EIMOR–HYDOR competition case (Fig. 2). One sees from Table I and Fig. 1 that this situation is sensitive to j_0. By means of varying r_{ex} one should be able to vary the EIMOR vs the HYDOR effects. Typical results are shown in Table II. One expects[1] that $J(r)$ will, at most, have a range of appreciable interaction equal to or slightly greater than d (i.e., $r_{ex}/d \sim 1$), so we first considered such reasonable variations of r_{ex}. One finds that an increase in r_{ex}, which according to the model enlarges the EIMOR, creating more EIMOR–HYDOR competition, does indeed lead to the predicted decrease in polarization. For the contact-exchange model [where $J(y_i) = J_0$ $i = 0$ and 0 for $i > 0$] one expects the minimum EIMOR–HYDOR competition and maximum polarization, and this is found. In our results, as long as $y_{ex} \lesssim 2.5$, the variation in the polarization due to the EIMOR effect is only about 4%. However, one can induce major effects by using a very large value of y_{ex} (where $\tau_1(\lambda)D/d^2 \gg 1$). In this case the EIMOR effect becomes dominant and the polarization becomes large and negative. Such a result is qualitatively similar to a model previously used[6,7] in which $J(r) = J_0$ a constant independent of r. These results even yield an artificial "polarization turnover"[3,4] (for $\Delta g = 0$) as one sweeps from lower to higher magnetic fields. They clearly emphasize the role of EIMOR–HYDOR competition when compared to the results for the more realistic cases. However, one should note that in cases where there are hyperfine interactions from many nuclei, this could lead to the situation that neither $S - T_\pm$ transition will be clearly favored in the HYDOR (unlike the simple case studied here) and thus one could have such a "polarization turnover," but one must recognize its different cause.

While we plan to discuss effects for $\Delta g \neq 0$ elsewhere, we note that for large values of $a \sim 0.1$, one finds that $\Delta g \neq 0$ causes only small effects on $\Delta\mathcal{F}^*$ at low fields (0–100 G), but at high fields it can produce significant

TABLE II. $\Delta\mathfrak{F}^* \times 10^3$ ($\mathfrak{F}^* \times 10^3$).[a]

B_0 (Gauss)	$r_{ex}/d = 0.5$	$r_{ex}/d = 1.0$	$r_{ex}/d = 2.0$	$r_{ex}/d = 2.5$	Other models: Contact exchange	Other models: $J(r) = J_0$ constant
20	3.19(28.4)	3.17(28.4)	3.10(28.5)	3.07(28.5)	3.21(28.4)	−0.44(2.10)
40	2.50(25.8)	2.48(25.8)	2.43(25.8)	2.40(25.9)	2.51(25.8)	−1.02(2.46)
60	1.88(24.4)	1.87(24.4)	1.83(24.4)	1.81(24.4)	1.89(24.4)	−2.05(3.34)
100	1.21(23.2)	1.20(23.2)	1.18(23.2)	1.17(23.2)	1.22(23.2)	−11.34(12.4)
500	0.25(22.1)	0.25(22.1)	0.25(22.1)	0.25(22.1)	0.25(22.1)	−0.02(0.69)
1000	0.13(22.0)	0.13(22.0)	0.13(22.0)	0.13(22.0)	0.13(22.0)	+0.01(0.61)

[a]Finite difference results found using $A_a d^2/D = 0.064$, $J_0 d^2/D = -0.16$ (i.e., a case of EIMOR–HYDOR competition), $\Delta g = 0$, $(g_a + g_b) d^2/D = 6.4 \times 10^{-10}$, $\sigma = 10^{-15}$, $\Delta_I = 0.03125$, $\Delta_0 = 1.295$, $N = 50$, $r_{N/d} = 33593$, $kd^2/D = 10^{20}$ ($\Lambda \cong 1$) and triplet initial condition.

differences by $S - T_0$ mixing in the manner discussed in detail previously.[1]

We also wish to note that the quantity $\mathfrak{F}^*$, given in Table I, gives the reaction yield for $\Lambda = 1$ for T. I. One can obtain the quantity $\mathfrak{F}(\Lambda)$ defined by Eq. (2.11a) which gives the reaction yield for any value of Λ, from the computed $\mathfrak{F}_\pm^*$ [or $\mathfrak{F}^*$ and $\Delta\mathfrak{F}^*$, cf. Eqs. (2.11)] by means of Eq. (2.12). This information is, of course, very useful in studies of field-dependent recombination kinetics.[18]

IV. CIDEP RESULTS

The results in Table III can be used with Eq. (2.14) to calculate typical values of $P^\infty_{a(\pm)}$ and P^∞_b for CIDEP in low magnetic fields. These results can be extended by noting that:

$$P^\infty_{HF(\pm)}(A_a, J_0, \Delta g = 0) = -P^\infty_{HF(\pm)}(-A_a, -J_0, \Delta g = 0) \tag{4.1a}$$

and

$$P^\infty_{LF(\pm)}(A_a, J_0, \Delta g = 0) = -P^\infty_{LF(\mp)}(-A_a, -J_0, \Delta g = 0)\,, \tag{4.1b}$$

which may be explained by the symmetry of $\mathcal{H}(r)$ [i.e., $\mathcal{H}(A_a, J(r), \Delta g = 0) = -\mathcal{H}(-A_a, -J(r), \Delta g = 0)$]. Initially one notes that the low-field CIDEP polarizations, P^∞_b are typically not as large as those generated at high fields for comparable values of the other parameters.[1] However, substantial polarizations can indeed occur at low fields particularly via $P^\infty_{a(\pm)}$, which are closely related to the initial condition. The maximum low-field polarizations occur when j_0 is of the correct magnitude to enhance the $S(\pm) \rightarrow T_\pm(\mp)$ transitions (i.e., in the EIMOR). The $S(\pm) \rightarrow T_\pm(\mp)$ transitions create electron-spin polarization via actual electron-spin flips, which deplete one of the $T_\pm(\mp)$ states relative to the other [cf. Fig. 2 and Eq. (2.14)]. Also, while it is true that at high fields $P^\infty_a(\Delta g = 0) = 0$, since the effects of $S - T_0$ exactly cancel [cf. Eq. (2.16a)], this is no longer true at low fields. This is because the two $T_\pm(\mp) \rightarrow S(\pm)$ transition rates are unequal [and they are unequal to the two unequal $T_\pm(\mp) \rightarrow T_0(\pm)$ rates] as a result of the differences in $E^{(1)}$ [cf. Eqs. (3.1)] of all the six levels. Thus the two states $S(\pm)$ are populated unequally by such transitions [and the two levels $T_0(\pm)$ which are initially equally populated for T. I. couple differently to the $T_\pm(\mp)$ states, so they adjust differently to the depopulating $T_0 \rightarrow S$ transitions]. Thus, the high-field type of $S \rightarrow T_0$ mixing leading to polarizations is significantly altered by these other low-field-active transitions, and it yields a nonzero contribution to P^∞_a. One can calculate from Table III the relative contributions of $P^\infty_{HF(+)} + P^\infty_{HF(-)}$ and $P^\infty_{LF(+)} + P^\infty_{LF(-)}$ to P^∞_a, finding that the latter usually accounts for about 50% of the total value of P^∞_a in the region $30 \lesssim B_0 \lesssim 100$G, but this percent increases as j_0 increases in the cases shown. Thus the $T_\pm(\mp) \rightarrow S(\pm)$ [and $T_\pm(\mp) \rightarrow T_0(\pm)$] transition followed by $S - T_0$ mixing does indeed provide significant contributions to the total result. The relative importance of this former effect is greatest (although the total polarizations are very small) at very low fields (i.e., $B_0 \lesssim 10$ G) and $j_0 \gg 1$ where P^∞_a becomes negative (i.e., emissive) for $a > 0$. But, as B_0 is increased, the role of the $T_-(-) \rightarrow S(+)$ transition (for $j_0 > 0$, cf. Fig. 2) becomes dominant yielding substantial positive values for P^∞_a (i.e., absorption). When $j_0 > 0$, the dominant $T_-(+) \rightarrow S(-)$ coupling (cf. Fig. 2) causes a negative P^∞_a, so it acts in cooperation with the $S \rightarrow T_0$ mixing effect. Figures 3 and 4 exhibit P^∞_a and P^∞_b vs magnetic field for some values of j_0.

Of course, the $T_\pm(\mp) \rightarrow S(\pm)$ transitions are quenched by high magnetic fields, and also $S - T_0$ effects cancel in P^∞_a and P^∞_b for $\Delta g = 0$ as noted above. CIDEP results for varying exchange distances, r_{ex}, in low magnetic fields revealed a complex functional dependence of polarization on $2J_0\tau_1(\lambda)$ that is similar to the case of high-field CIDEP [cf. Eqs. (3.14) and (3.17) of Ref. 1(a)]. Also, one must note that for the $\Delta g = 0$ case studies here, a contact exchange model yields results that are considerably different in magnitude than results for models of exchange with finite range, just as was found for high magnetic fields.

It is also possible for $T_\pm(\mp) \rightarrow S(\pm)$ transitions to play a significant role at high fields. This has been postulated as occurring in special systems.[11] Some of our calculations made for high fields but very viscous systems (cf. Table IV) do appear to be consistent with a recent discussion of experimental results[11c] provided $|j_0| \gtrsim 10^5$. Further studies of such high-field effects are planned.

In view of the possibility that the random T.I. condition may not always be appropriate, (cf. Ref. 15), we have also given some consideration to the effects on the polarizations of different initial conditions amongst triplet states. By the superposition principle[1]

TABLE III. CIDEP results.[a,b]

B_0 (Gauss)	$j_0 = 160.0$		$j_0 = 16.0$		$j = 1.6$	
	$P^{\infty}_{HF(+)} \times 10^3 / P^{\infty}_{HF(-)} \times 10^3$	$-P^{\infty}_{LF(+)} \times 10^3 / P^{\infty}_{LF(-)} \times 10^3$	$P^{\infty}_{HF(+)} \times 10^3 / P^{\infty}_{HF(-)} \times 10^3$	$-P^{\infty}_{LF(+)} \times 10^3 / P^{\infty}_{LF(-)} \times 10^3$	$P^{\infty}_{HF(+)} \times 10^3 / P^{\infty}_{HF(-)} \times 10^3$	$-P^{\infty}_{LF(+)} \times 10^3 / P^{\infty}_{LF(-)} \times 10^3$
0	−37.33/37.33	43.11/43.11	−40.41/40.41	42.08/42.08	−43.73/43.73	40.98/40.98
1	−37.05/37.45	43.11/42.98	−39.84/40.79	41.89/42.17	−43.31/44.02	40.70/41.11
5	−35.36/36.22	41.58/41.04	−38.29/39.60	40.02/40.66	−41.76/42.40	38.62/39.63
10	−31.51/32.37	37.02/36.41	−34.80/35.68	35.29/36.36	−37.67/37.77	33.73/35.12
15	−26.86/27.48	31.25/30.82	−30.48/30.78	29.51/30.97	−32.49/32.16	27.92/29.43
20	−22.44/22.79	25.68/25.49	−26.30/26.12	24.04/25.73	−27.49/26.90	22.52/23.97
25	−18.69/18.82	20.93/20.94	−22.71/22.22	19.44/21.22	−23.25/22.52	18.04/19.36
30	−15.68/15.66	17.10/17.25	−19.81/19.12	15.77/17.55	−19.86/19.08	14.51/15.68
35	−13.32/13.19	14.09/14.34	−17.52/16.73	12.90/14.63	−17.20/16.43	11.78/12.81
40	−11.47/11.27	11.73/12.03	−15.72/14.88	10.67/12.32	−15.14/14.38	9.68/10.58
45	−10.01/9.78	9.88/10.21	−14.30/13.44	8.93/10.48	−13.53/12.80	9.05/8.84
50	−8.86/8.60	8.41/8.75	−13.17/12.32	7.56/9.01	−12.25/11.57	6.78/7.47
55	−7.94/7.67	7.23/7.58	−12.26/11.43	6.47/7.82	−11.24/10.59	5.77/6.38
60	−7.19/6.92	6.27/6.62	−11.53/10.72	5.59/6.85	−10.43/9.81	4.96/5.50
65	−6.58/6.31	5.49/5.83	−10.92/10.15	4.87/6.05	−9.76/9.17	4.30/4.79
70	−6.08/5.82	4.85/5.18	−10.43/9.68	4.28/5.38	−9.21/8.66	3.76/4.20
75	−5.66/5.40	4.31/4.63	−10.01/9.29	3.78/4.82	−8.76/8.23	3.32/3.71
80	−5.31/5.06	3.85/4.16	−9.66/8.97	3.37/4.35	−8.37/7.87	2.94/3.30
85	−5.01/4.76	3.46/3.76	−9.36/8.70	3.02/3.94	−8.05/7.57	2.63/2.95
90	−4.75/4.52	3.13/3.42	−9.10/8.47	2.72/3.59	−7.77/7.32	2.36/2.65
95	−4.53/4.30	2.85/3.12	−8.88/8.27	2.46/3.28	−7.53/7.10	2.13/2.40
100	−4.34/4.12	2.60/2.86	−8.69/8.10	2.24/3.02	−7.32/6.91	1.93/2.17
150	−3.31/3.15	1.25/1.43	−7.64/7.22	1.04/1.54	−6.21/5.92	0.88/1.00
$>10^3$	−2.37/2.37	0.0/0.0	−6.76/6.76	0.0/0.0	−4.99/4.99	0.0/0.0

B_0 (Gauss)	$j_0 = 0.16$		$j_0 = 0.016$	
	$P^{\infty}_{HF(+)} \times 10^3 / P^{\infty}_{HF(-)} \times 10^3$	$-P^{\infty}_{LF(+)} \times 10^3 / P^{\infty}_{LF(-)} \times 10^3$	$P^{\infty}_{HF(+)} \times 10^3 / P^{\infty}_{HF(-)} \times 10^3$	$-P^{\infty}_{LF(+)} \times 10^3 / P^{\infty}_{LF(-)} \times 10^3$
0	−41.93/41.93	41.58/41.58	−41.69/41.69	41.66/41.66
1	−41.82/41.89	41.48/41.52	−41.61/41.62	41.58/41.58
5	−40.01/40.06	39.61/39.72	−39.77/39.78	39.73/39.74
10	−35.26/35/25	34.77/34.92	−34.95/34.95	34.90/34.92
15	−29.44/29.39	28.90/29.06	−29.08/29.07	29.02/29.04
20	−23.96/23.88	29.37/23.53	−23.54/23.53	23.48/23.50
25	−19.36/19.27	18.76/18.90	−18.92/18.91	18.86/18.87
30	−15.72/15.63	15.12/15.24	−15.26/15.25	15.20/15.21
35	−12.90/12.81	12.29/12.40	−12.42/12.41	12.36/12.37
40	−10.72/10.64	10.11/10.21	−10.23/10.23	10.17/10.18
45	−9.03/8.95	8.42/8.50	−8.53/8.52	8.47/8.48
50	−7.70/7.62	7.09/7.17	−7.20/7.19	7.14/7.14
55	−6.65/6.57	6.04/6.11	−6.14/6.13	6.08/6.09
60	−5.80/5.73	5.20/5.25	−5.29/5.28	5.23/5.24

TABLE III (*Continued*)

B_0	$j=0.16$		$j=0.016$	
(Gauss)	$P^{\infty}_{HF(+)}\times10^3/P^{\infty}_{HF(-)}\times10^3$	$-P^{\infty}_{LF(+)}\times10^3/P^{\infty}_{LF(-)}\times10^3$	$P^{\infty}_{HF(+)}\times10^3/P^{\infty}_{HF(-)}\times10^3$	$-P^{\infty}_{LF(+)}\times10^3/P^{\infty}_{LF(-)}\times10^3$
65	−5.11/5.04	4.51/4.56	−4.60/4.60	4.54/4.55
70	−4.55/4.48	3.95/3.99	−4.04/4.03	3.98/3.98
75	−4.08/4.02	3.48/3.52	−3.57/3.56	3.51/3.51
80	−3.68/3.63	3.09/3.13	−3.17/3.17	3.11/3.12
85	−3.35/3.30	2.76/2.80	−2.84/2.84	2.78/2.78
90	−3.07/3.02	2.48/2.51	−2.56/2.55	2.50/2.50
95	−2.83/2.78	2.24/2.27	−2.32/2.31	2.26/2.26
100	−2.62/2.57	2.03/2.06	−2.11/2.10	2.05/2.05
150	−1.50/1.47	0.93/0.94	−0.99/0.99	0.94/0.94
$>10^3$	−0.53/0.53	0.0/0.0	−0.05/0.05	0.0/0.0

B_0	$j_0=-0.016$		$j_0=-0.16$		$j_0=-1.6$	
(Gauss)	$P^{\infty}_{HF(+)}\times10^3/P^{\infty}_{HF(-)}\times10^3$	$-P^{\infty}_{LF(+)}\times10^3/P^{\infty}_{LF(-)}\times10^3$	$P^{\infty}_{HF(+)}\times10^3/P^{\infty}_{HF(-)}\times10^3$	$-P^{\infty}_{LF(+)}\times10^3/P^{\infty}_{LF(-)}\times10^3$	$P^{\infty}_{HF(+)}\times10^3/P^{\infty}_{HF(-)}\times10^3$	$-P^{\infty}_{LF(+)}\times10^3/P^{\infty}_{LF(-)}\times10^3$
0	−41.64/41.64	41.68/41.68	−41.40/41.40	41.76/41.76	−38.69/38.69	42.66/42.66
1	−41.56/41.56	41.60/41.59	−41.35/41.28	41.70/41.65	−38.89/38.28	42.79/42.36
5	−39.72/39.71	39.76/39.75	−39.47/39.42	39.89/39.77	−36.71/36.36	41.26/40.13
10	−34.88/34.88	34.93/34.92	−34.57/34.58	35.07/34.89	−31.22/31.50	36.55/34.98
15	−29.00/29.00	29.05/29.03	−28.62/28.68	29.18/29.01	−24.81/25.52	30.61/28.93
20	−23.45/23.46	23.51/23.49	−23.03/23.11	23.62/23.46	−18.89/19.82	24.91/23.32
25	−18.82/18.83	18.88/18.86	−18.37/18.46	18.98/18.83	−14.01/15.01	20.10/18.67
30	−15.16/15.16	15.22/15.20	−14.69/14.78	15.30/15.17	−10.19/11.19	16.27/15.01
35	−12.32/12.33	12.38/12.37	−11.83/11.93	12.45/12.34	−7.25/8.21	13.28/12.18
40	−10.12/10.13	10.19/10.18	−9.63/9.72	10.25/10.15	−4.99/5.90	10.96/10.01
45	−8.42/8.43	8.48/8.47	−7.92/8.01	8.54/8.45	−3.24/4.09	9.15/8.32
50	−7.09/7.10	7.15/7.15	−6.58/6.66	7.19/7.12	−1.88/2.67	7.73/7.00
55	−6.03/6.04	6.09/6.08	−5.52/5.60	6.13/6.13	−0.80/1.54	6.60/5.96
60	−5.18/5.19	5.24/5.23	−4.67/4.74	5.27/5.27	+0.07/0.63	5.69/5.12
65	−4.49/4.50	4.55/4.54	−3.98/4.05	4.58/4.58	0.77/−0.11	4.95/4.44
70	−3.92/3.93	3.98/3.98	−3.41/3.47	4.01/4.01	1.34/−0.72	4.34/3.89
75	−3.45/3.46	3.51/3.51	−2.94/3.00	3.54/3.54	1.81/−1.23	3.83/3.43
80	−3.06/3.06	3.12/3.11	−2.55/2.60	3.14/3.14	2.20/−1.66	3.40/3.04
85	−2.73/2.73	2.79/2.78	−2.21/2.27	2.81/2.81	2.54/−2.02	3.05/2.72
90	−2.44/2.45	2.50/2.50	−1.93/1.98	2.52/2.52	2.82/−2.33	2.74/2.44
95	−2.20/2.21	2.26/2.26	−1.69/1.74	2.28/2.25	3.06/−2.59	2.48/2.20
100	−1.99/2.00	2.05/2.05	−1.48/1.53	2.07/2.04	3.27/−2.82	2.25/2.00
150	−0.88/0.88	0.94/0.94	−0.37/0.40	0.94/0.93	4.36/−4.06	1.03/0.91
$>10^3$	+0.05/−0.05	0.0/0.0	+0.53/−0.53	0.0/0.0	4.99/−4.99	0.0/0.0

TABLE III (*Continued*)

B_0 (Gauss)	$j_0 = -16.0$		$j_0 = -160.0$	
	$P^{\infty}_{HF(+)} \times 10^3 / P^{\infty}_{HF(-)} \times 10^3$	$-P^{\infty}_{LF(+)} \times 10^3 / P^{\infty}_{LF(-)} \times 10^3$	$P^{\infty}_{HF(+)} \times 10^3 / P^{\infty}_{HF(-)} \times 10^3$	$-P^{\infty}_{LF(+)} \times 10^3 / P^{\infty}_{LF(-)} \times 10^3$
0	−32.90/32.90	44.59/44.59	−34.59/34.59	44.02/44.02
1	−33.15/32.52	44.91/44.08	−34.63/34.44	44.21/43.67
5	−31.03/31.10	43.93/41.39	−32.76/33.12	43.00/41.29
10	−26.06/27.08	39.66/36.04	−28.38/29.23	38.63/36.28
15	−20.35/21.90	33.90/35.97	−23.24/24.25	32.87/30.44
20	−15.10/16.84	28.17/24.37	−18.43/19.42	27.21/24.97
25	−10.75/12.51	23.19/19.70	−14.41/15.30	22.33/20.36
30	−7.33/9.01	19.13/15.99	−11.21/11.99	18.36/16.66
35	−4.69/6.25	15.90/13.10	−8.71/9.40	15.22/13.75
40	−2.64/4.09	13.35/10.85	−6.77/7.37	12.74/11.47
45	−1.06/2.40	11.33/9.09	−5.26/5.79	10.79/9.67
50	+0.19/1.05	9.71/7.71	−4.06/4.54	9.23/8.25
55	1.17/−0.02	8.41/6.60	−3.11/3.54	7.97/7.10
60	1.96/−0.89	7.35/5.70	−2.35/2.73	6.95/6.17
65	2.60/−1.60	6.48/4.97	−1.72/2.08	6.11/5.41
70	3.13/−2.19	5.75/4.37	−1.21/1.53	5.42/4.78
75	3.56/−2.68	5.14/3.87	−0.78/1.08	4.83/4.25
80	3.92/−3.10	4.62/3.45	−0.43/0.71	4.34/3.81
85	4.23/−3.45	4.19/3.09	−0.12/0.39	3.92/3.42
90	4.49/−3.75	3.81/2.79	+0.13/0.11	3.56/3.10
95	4.71/−4.00	3.48/2.52	0.36/−0.12	3.24/2.82
100	4.90/−4.23	3.19/2.30	0.55/−0.33	2.97/2.58
150	5.90/−5.45	1.61/1.07	1.56/−1.41	1.47/1.24
$>10^3$	6.76/−6.76	0.0/0.0	2.37/−2.37	0.0/0.0

[a]FD results found using a random triplet initial condition, $a = 0.064$, $y_{ex} = 1.0$, $\Delta g = 0$, $(g_a + g_b)d^2/D = 6.4 \times 10^{-10}$, $k = 0$ ($\Lambda = 0$), $N/d = 33953$, $N = 50$, $\Delta_I = 0.03125$, and $\Delta_0 = 1.295$.
[b]Positive polarizations, $P^{\infty}_a(\pm)$ and P^{∞}_b, indicate an ESR absorption signal will be observed, while negative polarizations yield an ESR emission signal.

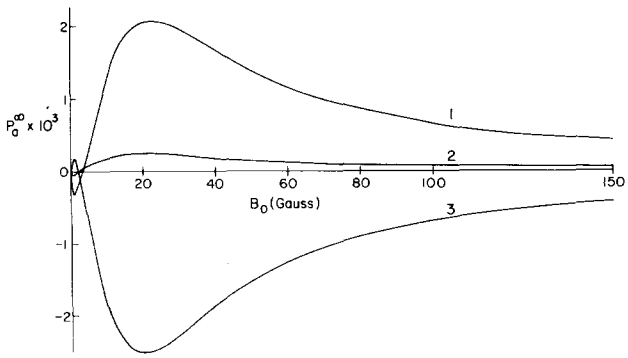

FIG. 3. $P_a^\infty \times 10^3$ as a function of the magnetic field, B_0, that is present. Curves 1–3 represent results calculated for $j_0 = 1.6$, 0.16, and -1.6, respectively. Other input parameters used in these calculations are $a = 0.064$, $y_{ex} = 1.0$, $\Delta g = 0$, $(g_a + g_b)d^2/D = 6.4 \times 10^{-10}$, $r_N/d = 33593$, $N = 50$, $\Delta_I = 0.03125$, $\Delta_0 = 1.295$, $k = 0$ ($\Lambda = 0$), $\sigma = 10^{-15}$ and a random triplet initial condition.

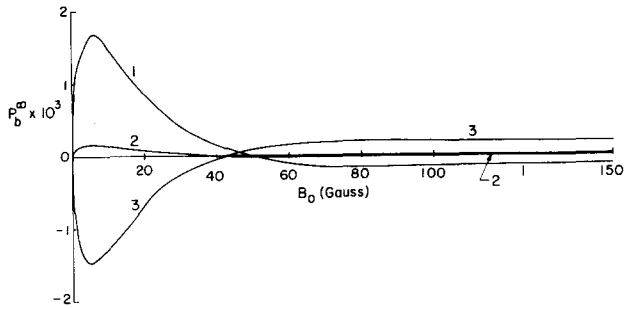

FIG. 4. $P_b^\infty \times 10^3$ as a function of the magnetic field, B_0, that is present. Curves 1–3 exhibit the calculated results for $j_0 = 1.6$, 0.16, and -1.6, respectively. Other parameters used in the calculation of P_b^∞ are $a = 0.064$, $y_{ex} = 1.0$, $\Delta g = 0$, $(g_a + g_b)d^2/D = 6.4 \times 10^{-10}$, $r_N/d = 33593$, $N = 50$, $\Delta_I = 0.03125$, $\Delta_0 = 1.295$, $k = 0$ ($\Lambda = 0$), $\sigma = 10^{-15}$, and a random triplet initial condition.

any particular T.I. condition may be obtained provided one computes the results of several special cases. Thus for example for CIDEP we may write:

$$P^\infty_{a(\pm)} = \rho_{T_0(\pm)}(t=0)\,P^\infty_{a(\pm)}[T_0(\pm)] + \rho_{T_+(\pm)}(t=0)\,P^\infty_{a(\pm)}[T_+(\pm)] + \rho_{T_-(\pm)}(t=0)\,P^\infty_{a(\pm)}[T_-(\pm)] \tag{4.2}$$

with similar expressions for $P^\infty_{b(\pm)}$. Here $P^\infty_{a(\pm)}[T_0(\pm)]$, etc. correspond to the $P^\infty_{a(\pm)}$ developed when initially all triplets are in the $T_0(\pm)$, etc. states, and $\rho_{T_0(\pm)}(t=0)$, etc. correspond to the actual initial values of these diagonal density-matrix elements. For the radical-pair mechanism discussed here we have noted that

$$P^\infty_{a(-)}[T_-(-)] = -P^\infty_{a(+)}[T_+(+)] = 1 \tag{4.3}$$

which may be used to simplify Eq. (4.2) to

$$P^\infty_{a(\pm)} = \rho_{T_0(\pm)}(t=0)\,P^\infty_{a(\pm)}[T_0(\pm)] + \rho_{T_\mp(\pm)}(t=0)\,P^\infty_{a(\pm)}[T_\mp(\pm)] \mp \rho_{T_\pm(\pm)}(t=0)\ . \tag{4.4}$$

Typical results indicate that any initial polarizations (e.g., $\rho_{T_+(+)} - \rho_{T_-(-)} \neq 0$ at $t=0$) which may have been generated by the triplet mechanism[1,15] are not greatly affected by the low-field radical-pair type mechanism.[19] Thus to a good approximation one can still consider the contributions of the triplet mechanism as independent of the radical-pair mechanism *provided* these contributions are large. But, if for example, $\rho_{T_-(\pm)} - \rho_{T_+(\pm)}$ is not large, then the low field results are significantly modified by the combined triplet and radical pair mechanisms.[19]

V. CONCLUSIONS

(1) By means of the modified FD equations used here, which lead to order-of-magnitude reductions in the size of the matrix to be inverted, it was feasible to obtain numerical solutions on a minicomputer to the SLE for a simple low-field case involving a single nucleus. This method (also in conjunction with other procedures[2]) should readily allow for the solution of more complex

TABLE IV. CIDEP in viscous systems.[a]

Additional input					
$\Delta g d^2/D$[b]	j_0	$P^\infty_{a(+)}$	$P^\infty_{a(-)}$	P^∞_a	P^∞_b
	10^4	15.33(15.43)	−15.32(−15.43)	0.01(0.0)	−0.01(0.0)
	10^5	13.20(13.75)	−8.48(−13.75)	4.72(0.0)	5.54(0.0)
0	10^6	12.49(12.50)	−11.71(−12.50)	0.79(0.0)	0.88(0.0)
	-10^5	−18.57(−13.75)	13.21(13.75)	−5.35(0.0)	−4.53(0.0)
	-10^6	−13.38(−12.50)	12.48(12.50)	−0.89(0.0	−0.74(0.0)
	10^4	15.85(15.98)	−13.86(−14.04)	1.99(1.95)	−1.99(−1.95)
	10^5	13.62(14.22)	−7.40(−12.41)	6.22(1.81)	+3.78(−1.81)
8×10^{-9}	10^6	13.01(13.32)	−9.43(−10.81)	3.57(2.51)	−1.94(−2.51)
	-10^5	−19.14(−14.22)	12.03(12.41)	−7.11(−1.81)	−3.07(+1.81)
	-10^6	−13.91(−13.32)	10.20(10.81)	−3.71(−2.51)	2.04(2.51)

[a]FD results found using $a = 640.0$, $(g_a + g_b)d^2/D = 6.4 \times 10^{-6}$, $y_{ex} = 1$, $k = 0$ ($\Lambda = 0$), $\sigma = 10^{-15}$, $B_0 = 3500$ G, $r_N/d = 33593$, $N = 50$, $\Delta_I = 0.03125$, $\Delta_0 = 1.295$ with Δg and j_0 as shown. The correct result which includes all couplings between the four states (S, T_0, T_+, T_-) is listed first. Following in parentheses is the result obtained from a $S - T_0$ (two state) coupling model. Results are for random T.I. This input would, for example, apply to the case where $d = 4$ Å, $D = 1 \times 10^{-9}$ cm^2/sec, $B_0 = 3500$ G, $A_a = 4 \times 10^8$ sec^{-1}, $(g_a + g_b) = 4.0$ with $\Delta g = 0$ or 0.005 and $J_0 = 0.625 \times 10^{10}$ sec^{-1}, $\pm 0.625 \times 10^{11}$ sec^{-1} or $\pm 0.625 \times 10^{12}$ sec^{-1}.

[b]For $\Delta g = 0$ and $a = 640.0$, $Qd^2/D = 160.0$ and -160.0 in the (+) and (−) manifolds, respectively. When $\Delta g d^2/D = 8 \times 10^{-9}$, Qd^2/D(+ manifold) = 283.12 and Qd^2/D (− manifold) = −36.88.

cases for CIDN(E)P as well as magnetic field effects on chemical reactivity.

(2) The low-field CIDNP and CIDEP results discussed here show a significant dependence upon the exchange interaction $J(r)$, in particular in terms of its range and its extent, which was not adequately dealt with by earlier more approximate theoretical analyses.

(3) All the computed results may be understood qualitatively in terms of a simple model involving both an outer region of r space, in which the hyperfine terms induce $T_{\pm} \rightarrow S$ transitions (HYDOR), and an inner region, in which $J(r)$ modulates the effectiveness of these transitions (EIMOR).

[1](a) J. H. Freed and J. Pedersen, Adv. Mag. Res. **8**, 1 (1976); (b) J. Pedersen and J. H. Freed, J. Chem. Phys. **57**, 1004 (1972); (c) **58**, 2746 (1973); (d) **59**, 2869 (1973); (e) **61**, 1517 (1974); (f) **62**, 1706 (1975). In these works the device of using two or three different values of the internodal separation was used.

[2]J. H. Freed in *Chemically Induced Magnetic Polarization*, edited by L. Muus *et al.* (Reidel, The Netherlands, 1977). Note: typographical errors may be corrected by inserting $\langle S, M_I \mid \mathcal{H}(r) \mid T_+, M_I - 1\rangle = \langle T_+, M_I - 1 \mid \mathcal{H}(r) \mid S, M_I\rangle = -B^-$.

[3]J. Pedersen, J. Chem. Phys. **67**, 4099 (1977). These ideas have also been discussed in the context of low-field CIDNP [J. Pedersen, Chem. Phys. Lett. **52**, 333 (1977)].

[4]F. Sarvarov *et al.*, Chem. Phys. **16**, 41 (1976).

[5]F. Adrian, Chem. Phys. Lett. **10**, 70 (1971).

[6]J. Morris *et al.*, J. Am. Chem. Soc. **94**, 2406 (1972).

[7]R. Kaptein and J. denHollander, J. Am. Chem. Soc. **94**, 6269 (1972).

[8]G. Evans and R. Lawler, Mol. Phys. **30**, 1085 (1975).

[9](a) R. Sagdeev *et al.*, Chem. Phys. Lett. **46**, 343 (1977); (b) D. Nelson, J. Phys. Chem. **82**, 1400 (1978).

[10](a) J. Garst *et al.*, J. Am. Chem. Soc. **92**, 5761 (1970); (b) J. Garst and R. Cox, *ibid.* **92**, 6391 (1970).

[11](a) A. Trifunac and D. Nelson, J. Am. Chem. Soc. **99**, 289 (1977); (b) A. Trifunac and D. Nelson, Chem. Phys. Lett. **46**, 376 (1977); (c) A. Trifunac, *ibid.* **49**, 457 (1977).

[12]Thus x of Ref. 1 obeys $x = y - 1$.

[13]G. P. Zientara and J. H. Freed, J. Chem. Phys. (to be published).

[14]We continue to neglect the effects of relaxation due to intermolecular electron–electron dipolar interactions which, like $J(r)$, are modulated by the relative translational diffusion of the radicals.[1] de Kanter *et al.* [Mol. Phys. **34**, 857 (1977)] have included them in an approximate manner for the biradical problems, where the two radical ends are in close proximity. For the radical-pair mechanism discussed here, the radicals are well-separated most of the time, so their effects should be small and any initial effects of the dipolar interaction prior to initial separation of the radical pair are more properly included in a consideration of the triplet polarization mechanism [cf. Refs. 15 and 1(a)]. It should be noted, however, that one may rigorously include effects of the dipolar interaction into the present model by writing the complete three-dimensional SLE where the diffusion operator Γ_r includes the angular dependence as well as the radial (r) dependence [cf. 1(a) and L. P. Hwang and J. H. Freed, J. Chem. Phys. **63**, 4017 (1975)] and then using an eigenfunction expansion[2] of the density matrix in angular variables. One then finds, by a simple perturbation analysis in the angular variables, expressions for T_1 and T_2 due to the dipolar mechanism, which are formally identical to those of relaxation by *rotational* modulation of a dipolar interaction, but now involve an explicit r dependence. That is, one obtains the results [cf. A. Abragam, *The Principles of Nuclear Magnetism* (Oxford University, New York, 1961), p. 300] that $J^{(p)}(\omega, r) = (p^2/r^6)\,\frac{4}{15}\,(\tau_2(r)/1 + \omega^2 p^2 \tau_2(r)^2)$ with $p = 1$ or 2 and where $\tau_2(r) \equiv r^2/6D$ with $D = D_1 + D_2$ the *translational* diffusion coefficient for the relative motion. These spectral densities are then inserted into the conventional expressions for T_1 and T_2 (cf. Abragam, above reference) to obtain r-dependent "quasirotational" $T_1(r)$ and $T_2(r)$, which should then be inserted into the SLE written for the restricted r space used in Refs. 1 and the present work.

[15]The T. I. condition we are using here might more properly be called random triplet initial. It is what has typically been used by others.[6–8] It corresponds to the simple case in which the lab-frame T_0, $T_{\pm}$ states are equally populated, even by preferential population of the low-field molecular frame T_x', T_y', T_z' states, since these states are randomly distributed in space. However, it is known [cf. Ref. 1(a), 1(f)] that the zero-field splitting in conjunction with the Zeeman energies of the triplet levels can, under appropriate conditions, lead to (sometimes large) initial polarizations in which $\rho_{T_-} - \rho_{T_+} \neq 0$, (i.e., the triplet mechanism [cf. Refs. 1(a) and 2, Chap. XI by P. W. Atkins]. Under such conditions it is no longer fully appropriate to use the random T. I. condition for the radical-pair mechanism (RPM) discussed in this paper, since the RPM can modify such initial polarizations by means of induced $T_{\pm} \rightarrow S$ and $T_{\pm} \rightarrow T_0$ transitions, (cf. Ref. 19). However, the triplet mechanism is not favored by the low magnetic fields which would favor such transitions induced by the RPM.

[16]Had we considered only $S - T_0$ coupling (i.e., $P^{\infty}_{\mathrm{LF}(\pm)} = 0$), Eqs. (2.15) generate Eq. (3.22b) of Ref. 1(a) with the appropriate numerical factors accounting for the difference in initial conditions.

[17]High field studies showed that the exact functional form of $J(r)$ did not affect CIDN(E)P results significantly, provided the chosen form has a similar range of interaction [where $J(r) > 0$] as the usual exponential form.

[18](a) H. Werner, *et al.*, J. Chem. Phys. **67**, 646 (1977). These workers gave formulas similar to Eqs. (2.5)–(2.8) but used them in the manner of Ref. 1; (b) K. Schulten *et al.*, Z. Phys. Chem. **101**, 371 (1976); (c) R. Haberkorn, Chem. Phys. **19**, 165 (1977); **24**, 111 (1977); **26**, 35 (1977).

[19]Thus for one typical case of $a = 0.064$, $j_0 = 16$, $y_{ex} = 1$, $B_0 = 35$ G, $\Delta g = 0$, $(g_a + g_b)d^2/D = 6.4 \times 10^{-10}$, $kd^2/D = 0$, one obtains $P^{\infty}_{a(+)}[T_-(+)] = 0.975290$ while $P^{\infty}_{a(-)}[T_+(-)] = -0.954933$ or only small changes from the $t = 0$ values of unity in each case. [One also finds that $P^{\infty}_{a(+)}[T_0(+)] = 52.409 \times 10^{-3}$, while $P^{\infty}_{a(-)}[T_0(-)] = 57.630 \times 10^{-3}$.] On the other hand the random T. I. yields $P^{\infty}_{a(+)} = 4.617 \times 10^{-3}$ from these above values, while other T.I. cases in which there is also no initial polarization lead to different results: E.g., (1) initial values of $\frac{1}{4}$ for $\rho_{T_{\pm}(\pm)}$ and $\rho_{T_-(\pm)}$ yields $P^{\infty}_{a(+)} = -6.25 \times 10^{-3}$; (2) initial values of $\frac{1}{2}$ for $\rho^{\infty}_{T_0(\pm)}$ yields $P^{\infty}_{a(+)} = 26.2 \times 10^{-3}$. Although cases (1) and (2) may not be realistic, they do emphasize the sensitivity of the RPM results to the choice of initial conditions. Other typical cases yield similar results.